Green Chemistry

Production of neo acids from biomass-derived monomers

Journal:	*Green Chemistry*
Manuscript ID	GC-ART-03-2023-000735.R1
Article Type:	Paper
Date Submitted by the Author:	05-Apr-2023
Complete List of Authors:	Andini, Erha; University of Delaware College of Engineering, Chemical and Biomolecular Engineering Bragger, Jake; University of Delaware College of Engineering, Chemical and Biomolecular Engineering Sadula, Sunitha; University of Delaware, Catalysis Center for Energy Innovation Vlachos, Dionisios; Univ. of Delaware,

Production of neo acids from biomass-derived monomers

Erha Andini,[1,2] Jake Bragger,[1] Sunitha Sadula,[2*] and Dionisios G. Vlachos[1,2*]

[1]Department of Chemical and Biomolecular Engineering, 150 Academy St., University of Delaware, Newark, Delaware 19716, USA
[2]Catalysis Center for Energy Innovation, 221 Academy St., University of Delaware, Newark, Delaware 19716, USA

*Corresponding author: vlachos@udel.edu and sunithak@udel.edu

Abstract

Neo acids are highly branched carboxylic acids currently produced from fossil fuels. In this work, we produce renewable neo acids from lignocellulosic biomass-derived furan and keto acids via C-C coupling through hydroxyalkylation/alkylation (HAA), followed by ring-opening of furans through hydrodeoxygenation (HDO). We show effective C-C coupling over acid catalysts. Catalyst screening and multi-parameter optimization using machine learning optimize the yield and elucidate the correlation between variables and outcomes. We demonstrate selective furan ring-opening without affecting the carboxylic acid to make neo acids using a co-catalyst involving Pd supported on carbon and metal triflate.

Keywords: Renewables, hydroxyalkylation/alkylation, hydrodeoxygenation, Koch synthesis, branched carboxylic acids, levulinic acid, furan

Introduction

The global population growth and improved quality of life have increased the demand for fuels, chemicals, and other products.[1,2] The increased agriculture and industrial manufacturing depend on fossil fuels. The associated environmental concerns demand renewable and sustainable alternatives. Lignocellulosic biomass, including forest wood, municipal solid waste, energy crops, and agriculture residue, is an abundant, renewable, non-edible promising alternative to fossil fuels. Recent advancements in conversion technologies of lignocellulosic biomass create unique opportunities to make valuable fuels and chemicals, such as lubricants, plastics, rubber, and detergents.[3–7]

Neo acids are highly branched *tert*-monocarboxylic acids commercially produced from fossil fuels. The high steric hindrance due to their structure imparts excellent thermal and hydrolytic stability, and resistance to chemicals and oxidative compounds. Their low pour point allows for easy transportation, storage, and handling.[8,9] Depending on the chemistry applied to the carboxylic functional group (reduction, dehydration, esterification, etc.), derivatives with diverse applications can be obtained, including polymers, adhesives, lubricants, agrochemicals, paints, coatings, and personal care products.[4,7,10–15] Neo acids are commercially manufactured from petroleum-derived olefins (isobutene and mixed nonenes) through the Koch synthesis (**Scheme 1**A&B),[8,16,17] such as neopentanoic acid and neodecanoic acid (ExxonMobil) and versatic acid (Hexion). However, the process involves harsh reaction conditions, such as high temperatures and pressures and strong acids, *e.g.,* H_2SO_4, HNO_3, H_3PO_4, HF, and toxic substances, which cause environmental concerns. Additionally, multi-step purifications are needed to separate dimeric and trimeric isobutene by-products. Thus, there remains a need for sustainable and environmentally friendly alternatives to produce neo acids from renewable resources, such as biomass.

Research into the chemical synthesis of branched carboxylic acids from biomass is still rare, with much attention on naturally occurring ones and microbial fermentation. Dembitsky presented a review of naturally occurring neo acids covering their identification in plants, algae, fungi, marine invertebrates, and microorganisms and isolation methods.[9] However, these processes are not economical and suffer from scalability issues. Microbial fermentation has been explored to produce branched carboxylic acids derived from biomass,[18–20] but the process is challenged by long fermentation time, selectivity, and enzyme inactivation. Li *et al*. described the chemical synthesis of medium-chain carboxylic acids from cellulose-derived platform chemicals (**Scheme 1**C).[21] However, the process uses a corrosive solvent, the products are straight-chain and iso carboxylic acids, and the chain length cannot be tailored. To the best of our knowledge, no reports on the catalytic synthesis of highly branched *tert*-monocarboxylic acids from biomass exist.

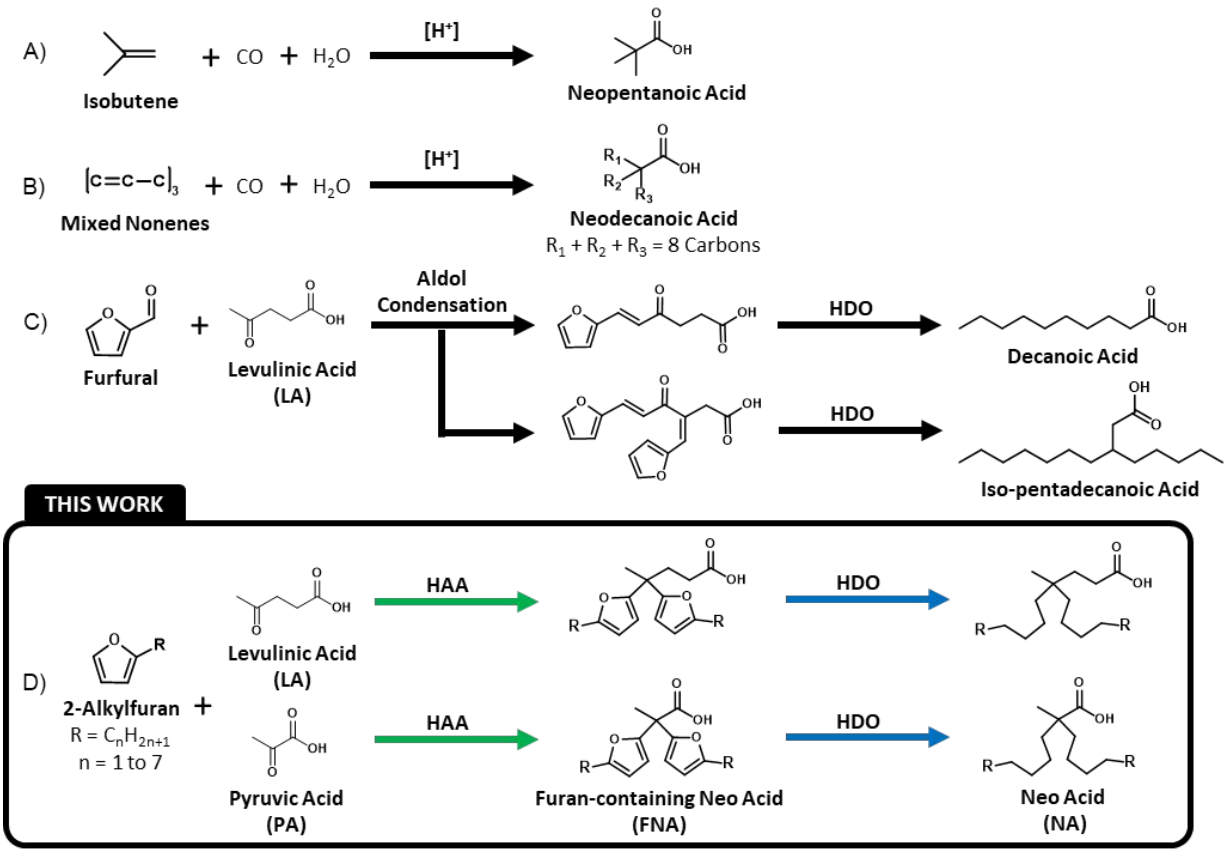

Scheme 1. Approaches to synthesize branched monocarboxylic acids. Industrial route to produce A) neopentanoic acid and B) neodecanoic acid. C) Chemical synthesis of medium-chain carboxylic acids from biomass. D) Our approach to renewable neo acids by hydroxyalkylation/alkylation (HAA) of 2-alkylfurans with levulinic acid (LA) or pyruvic acid (PA) followed by hydrodeoxygenation (HDO).

Here, we report a strategy to synthesize renewable neo acids with tailored molecular architecture from biomass-derived 2-alkylfuran and keto acids, *e.g.,* levulinic acid (LA) or pyruvic acid (PA), through C-C coupling of furans via hydroxyalkylation/alkylation (HAA) using a Brønsted acid catalyst followed by furan ring-opening (RO) via hydrodeoxygenation (HDO) using metal triflate and Pd/C (**Scheme 1**D). 2-alkylfuran with varying chain lengths can be produced through dehydration and HDO of biomass-derived C_5 sugars or furan acylation with valeric acid or valeric anhydride followed by HDO[7,22,23]. LA can be synthesized via dehydration of fructose followed by rehydration[24], and PA can be obtained via fermentation of glucose[25] (**Error! Reference source not found.**). While HAA chemistry has been reported to increase the carbon number of biomass-derived platform molecules and HDO chemistry has been reported for the RO of furan and other aromatic functionalities to make jet fuels, diesel, and lubricants from biomass,[26–33] the synthesis of highly branched carboxylic acids with tailored molecular architecture has not yet been reported. Wang *et al.* reported the HAA reaction between 2-methylfuran and angelica lactone (LA self-condensed product) producing renewable diesel with low yield (4.8%).[29] In our work, the HAA reaction successfully converts the reactants into furan-containing neo acids (FNA) and its ring opening (FNA RO) over Brønsted acid catalysts with more than 90% yield. Upon catalyst and

solvent screening, and optimization of the HDO step gives a 40% yield of the desired neo acid (C_{23}-NA) with 15% of iso acid (C_{14}-IA), a commercially valuable cracked product.

Results and discussion

Hydroxyalkylation/alkylation

Catalyst screening and product yield optimization

Different homogeneous and heterogeneous acid catalysts were evaluated using 2-pentylfuran (2-PF) as the model compound and levulinic acid under the reaction conditions of our previous work[34] (**Figure 1**). The acid catalysts included H_2SO_4, CH_3SO_3H, and *p*-TSA, hetero-poly acids (phosphotungstic acid (PTA), phosphomolybdic acid (PMA), and perfluorinated sulfonic acid resins (Aquivion PW79S and Aquivion PW98), commercial HY, and silica-alumina at equivalent acid (H^+) amounts. As shown in **Figure 1**A, all catalysts except HY zeolite and silica-alumina produced FNA as the main product and small fractions of other products *via* RO of the FNA (FNA RO) and self-condensation of 2-PF (SC-1, SC-2, SC-3, and SC-4) referred as PFSCs (**Figure 1**B). The conversions and yields are listed in **Error! Reference source not found.**. Water, a by-product of the condensation chemistry, likely facilitated the formation of FNA RO and PFSCs through acid-catalyzed hydrolysis and self-condensation, respectively. The mechanism of the HAA chemistry has been reported (**Error! Reference source not found.**).[34] The initial reaction rate data (**Error! Reference source not found.**) at various temperatures was used to estimate the apparent activation energies (E_a). An E_a of 34.3 kJ mol^{-1} was obtained. The performance was evaluated based on the combined yields of FNA and FNA RO, as FNA RO also produces neo acid upon HDO reaction. The catalytic performance follows the order of Aquivion PW79S > PTA > PMA > *p*-TSA > CH_3SO_3H > H_2SO_4 > Aquivion PW98 > HY. Silica-alumina shows no activity. Aquivion PW79S resulted in an overall FNA and FNA RO yield of 90% at a complete conversion of 2-PF and LA conversion of 82%. Blank experiments of 2-PF and LA alone over Aquivion PW79S (**Error! Reference source not found.**) confirm no self-condensation of 2-PF or LA. Aquivion PW79S was selected for the remaining experiments reported below.

While homogeneous acids, such as H_2SO_4, CH_3SO_3H, and *p*-TSA, give good overall yield (**Figure 1**A), they are corrosive and difficult to separate and recycle.[4,34–36] Amongst the heterogeneous catalysts, the overall yield of FNA and FNA RO can differ due to the catalyst's acid strength and density, surface area, and pore size (**Error! Reference source not found.**).[36,37] The high catalytic performance of Aquivion PW79S compared to the other acid catalysts can be attributed to its higher acid density, enabling higher accessibility of H^+ for the tandem C–C coupling reaction.[38,39] It is worth mentioning that the water by-product of HAA and the amphiphilic nature of perfluorinated sulfonic acid resin catalysts result in water clusters swelling the catalyst. Aquivion PW79S is more prone to swelling than Aquivion PW98 due to its higher acid density.[40,41] This phenomenon limits reactant accessibility to the active sites. The formation of water channels can be mitigated simply by performing reactions in a round bottom flask under high stirring speed (**Error! Reference source not found.**).

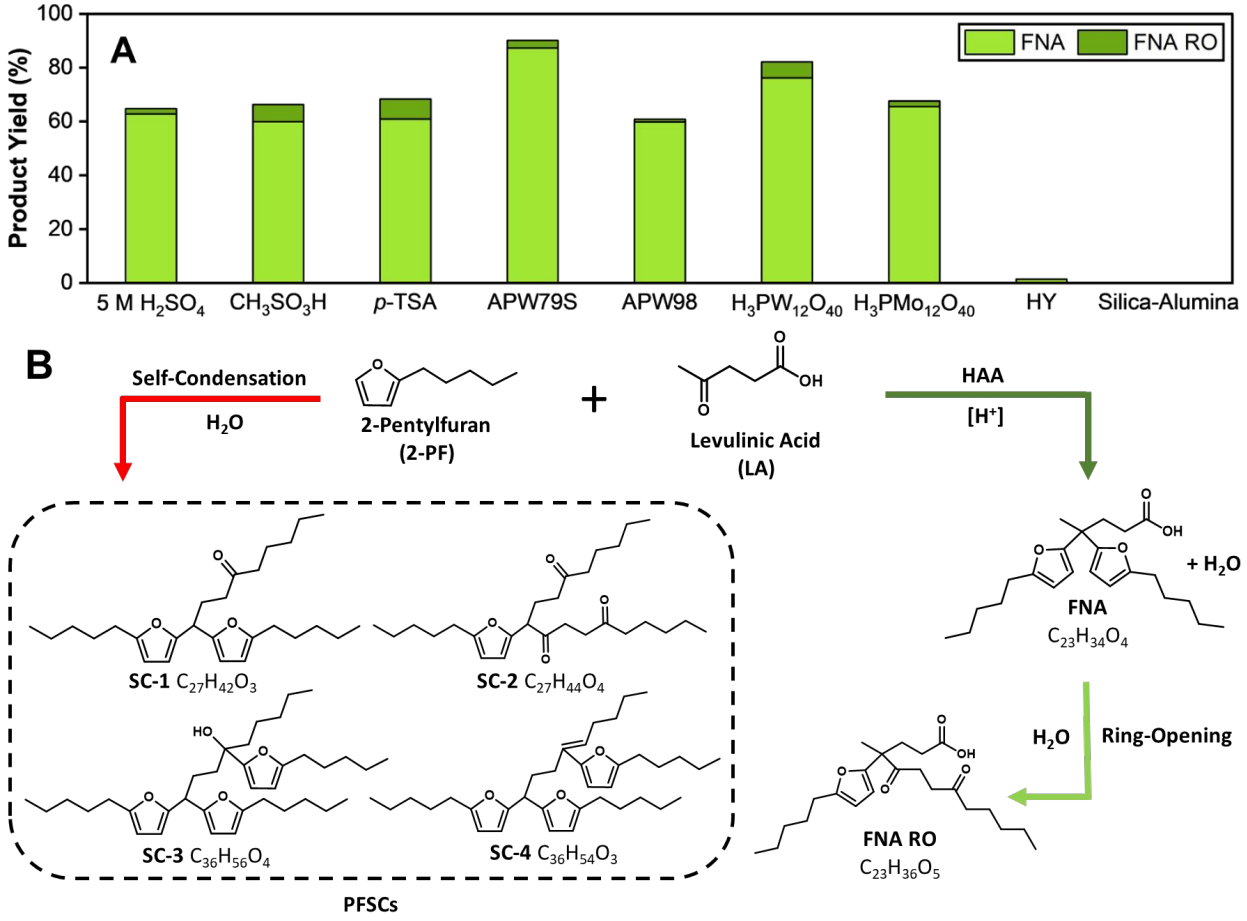

Figure 1. Reaction products from the HAA reaction of 2-pentylfuran and levulinic acid and catalysts screening results. A) Proposed reaction network for the formation of condensation products. B) FNA and FNA RO yield over various acid catalysts. Reaction conditions: 20 mmol 2-pentylfuran (2-PF), 10 mmol levulinic acid (LA), 0.107 mmol H^+ catalyst, 65°C, 6 h, 800 rpm.

Optimization of the operating conditions using active learning (see Methods) led to an overall yield of 90% at complete conversion of 2-PF and 82% conversion of LA under 2-PF/LA molar ratio of 2, Aquivion PW79S loading of 0.107 mmol H^+, a temperature of 65 °C, time of 6 h, and stirring speed of 800 rpm (**Error! Reference source not found.**). Analysis of the data using principal component analysis (PCA) shows revealed correlations among parameters (**Error! Reference source not found.**).

Extending the HAA chemistry to different 2-alkylfurans and ketones

The optimal reaction conditions were applied to other 2-alkylfurans and keto acids to obtain neo-acid precursors of varying chain length (**Table 1**). Pyruvic acid on average produces 10% more neo-acid precursor than levulinic acid likely due to the closer distance of the keto group to the –COOH group, resulting in an increase in reactivity due to a stronger electron withdrawing impact by the –COOH group. High overall yields of C_{13}-C_{27} FNA and FNA RO (47% to 92%, depending on the molecular sizes) over Aquivion PW79S were obtained, except for Entry 1. The substantially lower combined yield of FNA and FNA RO, when R is a methyl group (2-MF), is due to the self-

condensation of 2-MF. This is supported by the low conversion of levulinic acid (58%) even though almost all 2-MF is converted (**Error! Reference source not found.**). A low total carbon balance (75%) was also obtained after accounting all the peaks on the GC spectra, suggesting the formation of high-molecular weight molecules not detected by GC/GC-MS. A low kinetic barrier for self-condensation is possible.[42] Nonetheless, the data shows a promising route to synthesize neo-acid precursors with tunable structures.

Table 1. HAA reaction between different 2-alkylfurans and keto acid of varying molecular sizes. Reaction Conditions: 20 mmol 2-alkylfuran, (2-alkylfuran/keto acid) (mol/mol) = 2, 0.107 mmol H^+ Aquivion PW79S, 6 h, 65°C, 800 rpm.

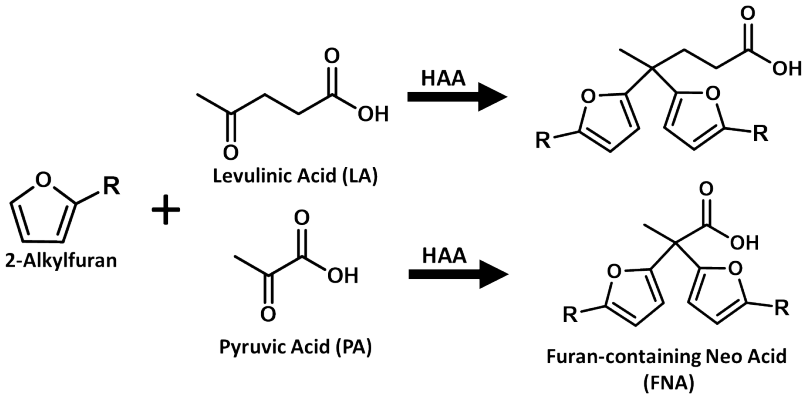

Entry	Reagents		#C	Yield FNA + FNA RO (%)	Total C Balance (%)
	R	Keto Acid			
1	Methyl	LA	C_{15}	47	75
2	Ethyl	LA	C_{17}	77	94
3	n-Propyl	LA	C_{19}	87	102
4	n-Butyl	LA	C_{21}	75	87
5	n-Pentyl	LA	C_{23}	90	101
6	n-Heptyl*	LA	C_{27}	82	89
7	Methyl	PA	C_{13}	86	93
8	Ethyl	PA	C_{15}	87	90
9	n-Propyl	PA	C_{17}	92	95
10	n-Butyl	PA	C_{19}	90	92
11	n-Pentyl	PA	C_{21}	86	89
12	n-Heptyl	PA	C_{25}	79	84

*Ten hours reaction time. #Carbon chain length

HAA catalyst recyclability

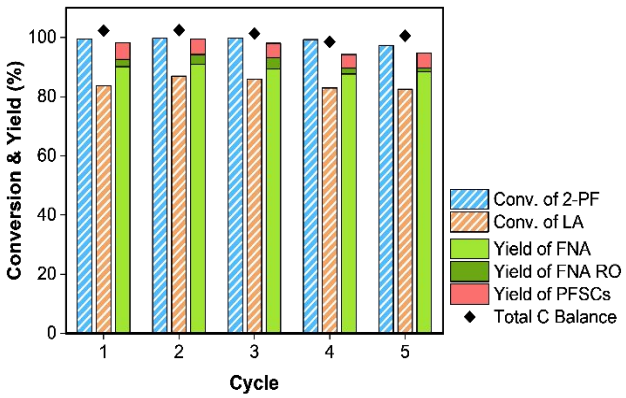

Figure 2. Recyclability of Aquivion PW79S in the HAA reaction of 2-pentylfuran and levulinic acid. Reaction conditions: 20 mmol 2-pentylfuran (2-PF), 10 mmol levulinic acid (LA), 0.107 mmol H^+ catalyst, 65°C, 6 h, 800 rpm.

For assessing catalyst recyclability, the liquid products were decanted out after each cycle. The catalyst was washed thrice with cyclohexane and ethyl acetate to remove surface-adsorbed unreacted reactants and products and then dried in a vacuum oven at 60 °C for 1 h before reuse in the next cycle. **Figure 2** shows that the catalyst achieves similar conversions and yields in five consecutive cycles. The slight decrease in LA conversion and product yields among cycles can be attributed to slight deactivation, likely due to covering some of the catalyst sites by adsorbed products. This is supported by FT-IR results on the spent catalyst showing additional bands at 2800–3000 cm^{-1} corresponding to C–H stretching (**Error! Reference source not found.**).

Hydrodeoxygenation

Catalyst screening

We adapted our previously furan ring-opening reaction conditions employed in the production of adipic acid[43,44] and decanoic acid[21]. Initially, we implemented Gilkey *et al.* and Tran *et al.* catalytic systems due to their promising results in selectively opening the tetrahydrofuran (THF) ring without impacting the carboxylic acid groups in making adipic acid. Hydrogenation was performed on the HAA product solution containing FNA, FNA RO, PFSCs and unreacted LA (after catalyst filtering) over Pd/C to saturate the furan ring. The reaction conditions were selected from our previous work.[4] The tetrahydrofuran-containing neo acid (THFNA) was successfully formed at nearly 95% yield but neo acid did not form in the ring opening step over Nafion and iodide salt (**Table 2**, entry 1). Ring opening of the hydrogenated product using $[MIM(CH_2)_4SO_3H]I$ ionic liquid[44] did not form a neo acid (**Table 2**, entry 2). The difference in the activity of tetrahydrofuran-based in our work and the tetrahydrofuran-2,5-dicarboxylic acid (THFDCA) in the literature is the two carboxylic acid groups that withdraw electrons facilitating the ring opening. Their absence makes ring-opening chemistry more challenging.

The HDO reactions using metal triflates and Pd/C catalysts[21] convert the HAA product solution into C_{23}-neo acid (C_{23}-NA). Here, Pd/C acts as a hydrogenation catalyst and metal triflate as the ring-opening catalyst. The HDO reaction also produced a cracked product, C_{14}-iso acid (C_{14}-IA). Nearly 30% of the total carbon was missing. The iso acids in the current process are commercially

valuable, *e.g.,* the isostearic acid is used widely in additives, emollients, hydraulic fluids, and personal care emollients.[45] Given the promising preliminary results, other metal triflates were screened and found that the higher the effective charge density on the metal cation, the higher the selectivity toward C_{23}-NA (**Table 2**, entries 5 - 16).[21,46] The highest yield was 37% C_{23}-NA and ~13% C_{14}-IA with $Al(OTf)_3$ and Pd/C co-catalyst. Although cerium and hafnium triflate have higher effective charge density than aluminum triflate, they yield lower neo acids. This could be due to their higher sensitivity to the water by-product compared to aluminum triflate.[47,48]

Table 2. Catalyst screening for the HDO of FNA and FNA RO.

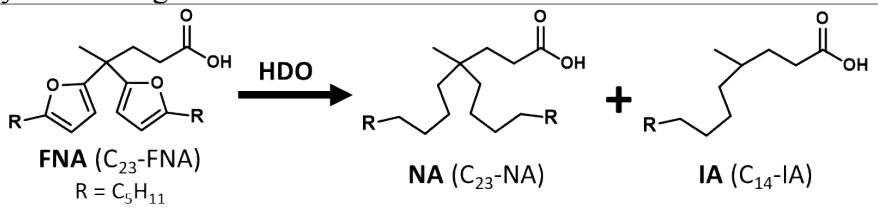

FNA (C_{23}-FNA) **NA** (C_{23}-NA) **IA** (C_{14}-IA)

Entry	Hydrogenation Catalyst	Promoter	Yield (%)	
			C_{23}-NA	C_{14}-IA
1[a]	-	Nafion + LiI	-	-
2[b]	-	$[MIM(CH_2)_4SO_3H]I$	-	-
3	Ru	$Al(OTf)_3$	-	-
4	Pt	$Al(OTf)_3$	21	11
5	Pd	$Al(OTf)_3$	37	13
6	Pd	$Hf(OTf)_4$	31	15
7	Pd	$Ce(OTf)_4$	20	1
8	Pd	$La(OTf)_3$	1	0
9	Pd	$Sm(OTf)_3$	0	2
10	Pd	$Eu(OTf)_3$	17	10
11	Pd	$Nd(OTf)_3$	1	12
12	Pd	$Sc(OTf)_3$	9	12
13	Pd	$Cu(OTf)_2$	14	9
14	Pd	$Sn(OTf)_2$	15	30
15	Pd	$Zn(OTf)_2$	1	9
16	Pd	Ag(OTf)	25	3

Reaction conditions: Entries 3-16 correspond to 1 mmol FNA, 6 mol% $M(OTf)_x$, 2 mol% hydrogenation catalyst, 10 mL n-octane, 3 MPa H_2, 180°C, 1 h, 500 rpm. Conversion ≥ 99% & total carbon balance ≤ 70%. [(a)] Entry 1 for hydrogenation reaction: 0.5 g HAA solution, 0.03 g Pd/C, 10 mL cyclohexane, 60°C, 2 h, 6 MPa H_2, 500 rpm. Pd/C was reduced under H_2 (50 mL/min) at 200°C for 1 h; Deoxygenation reaction: 1 wt% THFNA, 0.3 M H^+ Nafion, 0.3 M lithium iodide (LiI), 15 mL propionic acid, 160°C under 500 psi H_2, 2 h. [(b)] Entry 2: hydrogenation reaction as in (a) followed by deoxygenation reaction:

0.165 g THFNA (0.165 g), 1.55 g [MIM$(CH_2)_4SO_3H$]I, 2 h, 3.5 MPa H_2, 180°C, and 500 rpm.

Solvent screening

Different organic solvents were screened (**Figure 3**). A solvent-free reaction is not practical as the HAA solution is highly viscous. We found that non-polar organic solvents yield higher C_{23}-NA due to the better solubility of reactants, intermediates, and products without reacting with the metal triflate.[21] When a polar protic solvent, such as acetic acid, was used, esters and cracked products formed along with the neo acid. In polar aprotic solvents, such as ethyl acetate and THF, no reaction occurred likely due to deactivation of the metal triflate. According to Zhou *et al*.[47] and Keskiväli *et al*.[49], metal triflate with solvents bearing Lewis basic oxygen atoms ensued coordination between the metal center and the polar solvent, resulting in metal triflate deactivation. Mixtures of polar and non-polar organic solvents were explored to improve solvation of the substrates but no improvement in the C_{23}-NA yield.

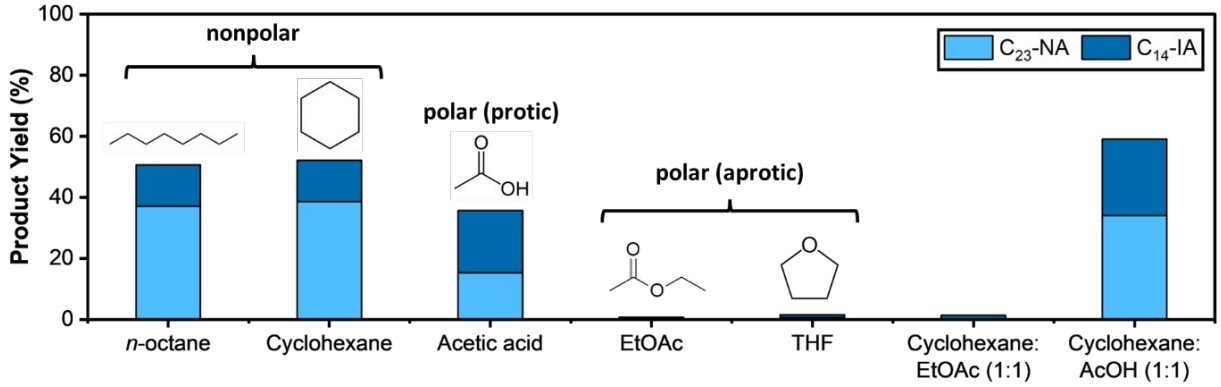

Figure 3. The effect of solvent on the HDO reaction. C23-NA is neo acid with 23 carbon atoms. C14-IA is iso acid with 14 carbon atoms. Reaction conditions: 1 mmol FNA, 6 mol% $Al(OTf)_3$, 2 mol% Pd/C, 10 mL solvent, 3 MPa H_2, 180°C, 1 h, 500 rpm.

Reaction parameter optimization

To investigate the role of hydrogenation catalyst and metal triflate on the HDO chemistry, control experiments were conducted with Pd/C alone and metal triflate alone and results are presented in **Table S6**. The GC chromatograms for each reaction are overlaid in **Error! Reference source not found.**. In the control reaction of $Al(OTf)_3$ alone, neither neo acid nor unreacted HAA products were observed, likely due to self-oligomerization of the starting materials facilitated by the metal triflate. This hypothesis is supported by the black color and turbid solution upon reaction (**Error! Reference source not found.B**) and high molecular weight species detected by LCMS (**Error! Reference source not found.**). Similarly, neither neo acid nor starting materials were observed over Pd/C alone. Instead, THFNA formed in quantitative yield (**Error! Reference source not found.C**), consistent with Pd's reported activity for furan ring-hydrogenation.[23] These control experiments confirm no self-condensation of the FNA and FNA RO being responsible for the missing carbon balance. These results also indicate that Pd/C and metal triflate are required to form neo acid.

The effect of varying catalyst molar ratio, hydrogen pressure, temperature, and time were also studied (**Figure 4**). We found that the HDO reaction required a suitable ratio of the hydrogenation catalyst (Pd/C) and metal triflate to form neo acid (**Figure 4A**). The yield of C_{23}-NA initially increased and then decreased with increasing the ratio of $Al(OTf)_3$. The same trend was observed with varying the Pd/C. We found that C_{23}-NA yield increases with increasing hydrogen pressure and plateaus above 3 MPa. The increase of hydrogen pressure ensures complete hydrogenation of the intermediates and final products, minimizing undesired side reactions and cracking, improving the yield of C_{23}-NA (**Figure 4B**). Under all reaction temperatures explored (150 – 220°C), the reactant was completely converted. With increasing reaction temperature, the yield of neo acid increased up to 180°C and then decreased (**Figure 4C**). These results suggest that at higher temperatures, the neo acid might undergo side reactions leading to high molecular weight species not detected by GC/GCMS. Lastly, a time-dependent study was conducted. At time zero, which is the pre-heating time, all the reactant has converted but no C_{23}-NA was detected. As the reaction proceeds, C_{23}-NA starts forming but plateaus after 30 min (**Figure 4D**). Parameter optimization leads to 40% yield of C_{23}-NA and 15% yield of C_{14}-IA at Pd/C:$Al(OTf)_3$ ratio of 2:6, 3 MPa H_2, 180°C, 30 min, and cyclohexane as the solvent.

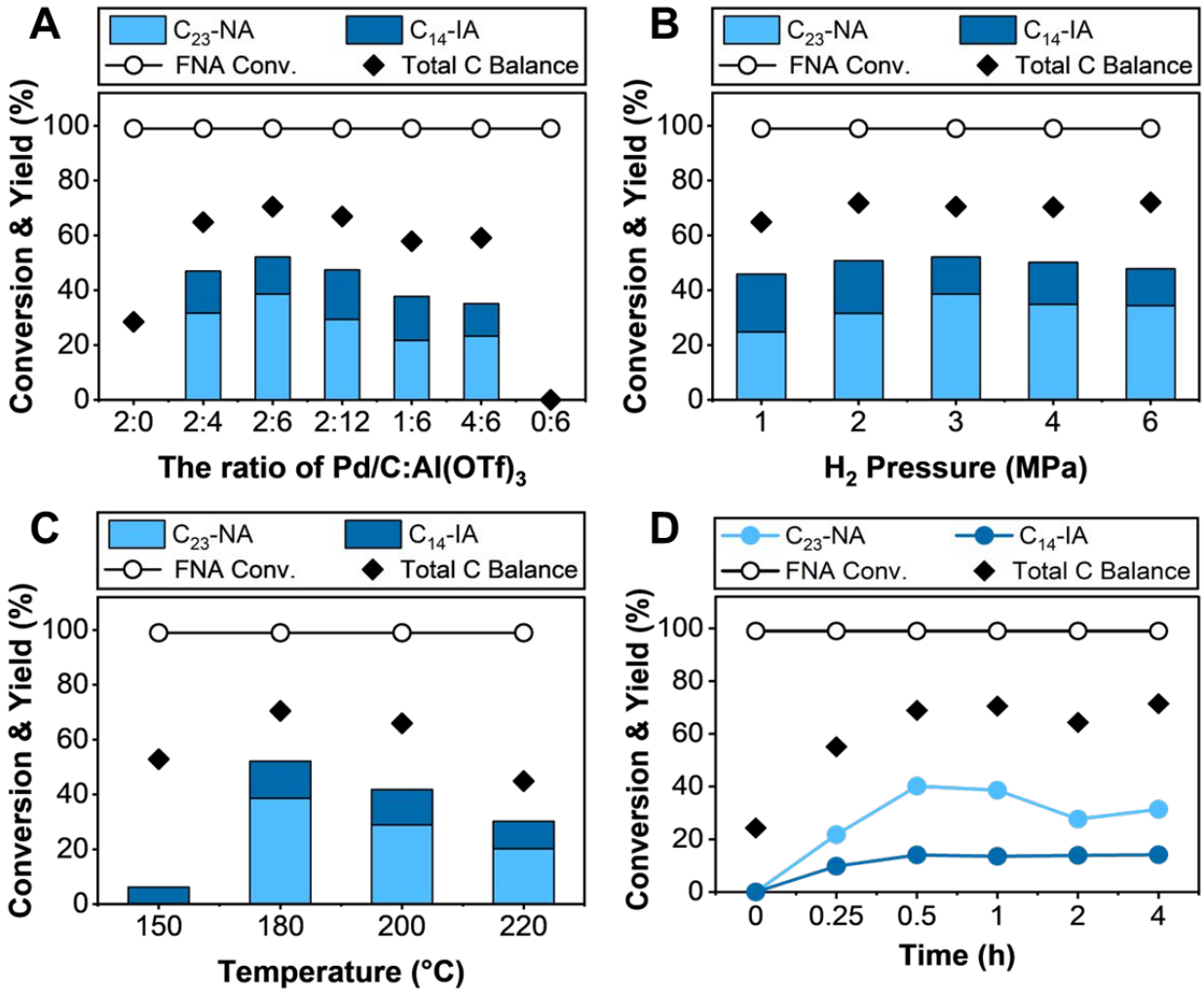

Figure 4. Effect of reaction parameters on product distribution for the HDO reaction. A) Catalyst molar ratio, B) H_2 pressure, C) Temperature, and D) Time. Reaction conditions: A) 1 mmol FNA, 10 mL cyclohexane, 3 MPa H_2, 180°C, 1 h, 500 rpm. B) 1 mmol FNA, 6 mol% $Al(OTf)_3$, 2 mol% Pd/C, 10 mL cyclohexane, 180°C, 1 h, 500 rpm. C) 1 mmol FNA, 6 mol% $Al(OTf)_3$, 2 mol% Pd/C, 10 mL cyclohexane, 3 MPa H_2, 1 h, 500 rpm. D) 1 mmol FNA, 6 mol% $Al(OTf)_3$, 2 mol% Pd/C, 10 mL cyclohexane, 180°C, 3 MPa H_2, 500 rpm.

To understand the plateau after 30 min, several hypotheses were tested. A certain amount of water was added to the reaction mixture at the optimized reaction conditions. The results confirmed no detrimental effect on neo acid production (**Error! Reference source not found.A**). FNA and HDO reaction intermediates could form high-molecular weight species, poisoning or blocking the active sites of the catalyst. Fresh catalyst added showed no improvements in product yields (**Error! Reference source not found.B**). To check if the side reactions from -COOH group cause the carbon loss, the -COOH group protection was performed by esterification of FNA with methanol, making furan-containing neo ester (FNE), which was then subjected to ring-opening (**Error! Reference source not found.**). All FNE converted at 1 h and yield of C_{24}-NE increases slowly with time, but the yields and total carbon balance were lower compared to FNA HDO (**Error! Reference source not found.**). These investigations and literature evidence[50] suggest that reactant and intermediates participate into side reactions.

Conclusions

Neo acids are commercially manufactured from petroleum derived olefins through the Koch synthesis under harsh reaction conditions using acids and multi-step purifications. Here, we demonstrated a strategy to synthesize renewable neo acids from biomass-derived 2-alkylfurans and keto acids through C-C coupling of the furans via hydroxyalkylation/alkylation (HAA) followed by ring-opening via hydrodeoxygenation (HDO) of furans. HAA reaction between 2-pentylfuran (2-PF) and levulinic acid (LA) produced furan based neo-acid precursors (FNA and FNA RO) in 90% yield over a solid acid catalyst. A 40% yield of the desired neo acids (C_{23}-NA) was obtained with 15% of C_{14}-NA product.

Experimental

Chemicals and materials

Aquivion® PW79S (coarse powder, Brunauer–Emmett–Teller (BET) surface area <1 m^2/g, and 1.26 mmol H^+/g), Aquivion® PW98 (coarse powder, BET surface area <1 m^2/g, and 1.0 mmol H^+/g), phosphotungstic acid hydrate (BET surface area <1 m^2/g and 1.04 mmol H^+/g), phosphomolybdic acid hydrate (BET surface area 1-5 m^2/g and 1.5 mmol H^+/g), amorphous silica alumina (ASA; catalyst support grade 135; 12 wt % Al_2O_3; >90% AS-100 mesh; pore size, 5.4 nm; BET surface area, 569 m2/g; and 0.34 mmol H+/g), 2-methylfuran (99%), 2-pentylfuran (≥98.0%), 2-ethylfuran (≥99.0%), levulinic acid (98%), pyruvic acid (98%), eicosane (99%), ethyl acetate (99.8%), acetic acid (≥99.7%), methanesulfonic acid (≥99.0%), *p*-toluenesulfonic acid monohydrate (≥98.5%), triflic acid (≥99.0%), $Eu(OTf)_3$ (98%), $La(OTf)_3$ (99%), $Nd(OTf)_3$ (98%), $Sc(OTf)_3$ (99%), $Cu(OTf)_2$ (99%), $Zn(OTf)_2$ (99%), Ag(OTf) (≥98%), $Sm(OTf)_3$ (98%), Pd/C (10 wt % Pd loading), Pt/C (10 wt % Pt loading), pyridine (99.8%), and N,O-Bis(trimethylsilyl)trifluoroacetamide (BSTFA) (≥99.0%) were purchased from Sigma-Aldrich.

Cyclohexane (99.9%) and methanol (≥99.9%) was purchased from Fisher Chemical. 2-Propylfuran (>98%) and 2-butylfuran (>98%) were purchased from Tokyo Chemical Industry Co. Ltd. HY (CBV720; Si/Al = 15; pore size, ~0.7 nm; BET surface area 780 m^2/g; and 0.31 mmol H^+/g) was purchased from Zeolyst. H_2SO_4 (5 M) was purchased from Fluka. Ru/C (10 wt % Ru loading) was purchased from Riogen. $Hf(OTf)_4$, $Al(OTf)_3$ (99%), $Ce(OTf)_4$ (98%), $Sn(OTf)_2$ (97%), and 2-heptylfuran (97%) were purchased from Alfa Aesar.

Materials Pretreatment

2-Alkylfurans (2-methylfuran, 2-ethylfuran, 2-propylfuran, 2-butylfruan, 2-pentylfuran, 2-hexylfuran and 2-heptylfuran) were purified by vacuum distillation before use.

Reaction procedures

Hydroxyalkylation/alkylation (HAA)

In a typical reaction, 20 mmol (2.76 g) 2-alkylfuran, 10 mmol (1.16 g) levulinic acid or 10 mmol (0.88 g) pyruvic acid, and a calculated amount of catalyst were mixed in a 50 mL round-bottom flask without any solvent. The flask was placed in a preheated oil bath and magnetically stirred at 800 rpm. The reaction was run at the desired temperature for a specified reaction period. After the reaction, the solution was diluted using 10 ml of cyclohexane and 5 mL ethyl acetate solvents. Ethyl acetate was used to solubilize unreacted levulinic acid. Eicosane (C_{20}) was added as an internal standard, and the catalyst was separated from the solution by syringe filtration.

Hydrodeoxygenation

HDO of FNA over metal triflate was performed in a 50-mL Parr reactor (4790 pressure vessel, Parr Instrument Company) with an inserted glass liner and a magnetic stirrer. First, 1 mmol (0.37 g) of FNA, 6 mol% (0.029 g) $Al(OTf)_3$, 2 mol% (0.021 g) of 10 wt% Pd/C, and solvent (10 mL of cyclohexane) were added to the reactor, and the reactor was sealed with the reactor head equipped with a thermocouple, a rupture disk, a pressure gauge, and a gas release valve. The reactor was purged with 1 MPa N_2 five times and followed by 1 MPa H_2 five times, and finally pressurized to the desired H_2 pressure. The reaction mixture was heated to the desired temperature with continuous stirring at 750 rpm. The heating time to reach the set temperature was about 20 min. Once the desired temperature was reached, the mixture was run for a specified reaction period. Upon completion, the reactor was immediately transferred to an ice bath, cooled to room temperature, and H_2 was released. The reaction solution was diluted using 5 mL of ethyl acetate with a small amount of decane (C_{10}) as an internal standard, and the catalyst was separated from the solution by filtration.

Derivatization technique

Silylation, a derivatization technique, was implemented to improve the chromatographic behavior of the polar neo acid compounds and intermediates. Silylation works by selectively replacing the active hydrogens on the compound with an alkylsilyl group, resulting in less polar and more volatile compounds and better separation in gas chromatography (GC).[51] In a typical reaction, 100 µL product, 900 µL solvent, 250 µL pyridine, and 250 µL BSTFA were mixed in a GC vial. Then, the solution was heated on a hot plate at 65°C for 20 minutes.

Analysis of products and catalyst

The products were analyzed using a gas chromatograph (Agilent 7890A) equipped with an HP-1 column and a flame ionization detector (FID). The products were identified by a GC (Agilent 7890B) mass spectrometer (MS, Agilent 5977A with a triple-axis detector) equipped with a DB-5 column, high-resolution MS with liquid injection field desorption ionization (LIFDI), ^{1}H nuclear magnetic resonance (NMR), and ^{13}C NMR (Bruker AV400, $CDCl_3$ solvent). Fourier transform infrared (FTIR) data was collected with a Thermo Fisher FTIR/ATR by scanning the sample from 400 to 4000 nm.

The conversion and yield of all products were calculated on a carbon basis using the following equations:

$$\text{Conversion (\%)} = \frac{\text{Moles of carbon converted}}{\text{Moles of carbon in initial reactant}} \text{x } 100\%$$

$$\text{Yield (\%)} = \frac{\text{Moles of carbon product}}{\text{Moles of carbon in initial reactant}} \text{x } 100\%$$

Computational methods

Multi-parameter optimization using NEXTorch

To maximize the reactants' conversion and product yield, a multi-parameter optimization was conducted using NEXTorch, a recently developed active learning-driven optimization toolkit in our group.[52] Reaction parameters, including temperature, time, molar ratio, and catalyst loading, influence the FNA selectivity. Many studies have reported optimization studies of HAA chemistry by changing one parameter at a time.[30,35,37,53] The one at the time approach prevents us from optimizing FNA yield by changing all parameters simultaneously and understanding correlations between parameters. The traditional factorial design of experiments (DOE) has been implemented for a long time[54,55] to optimize lab-scale production of fuels and chemicals from biomass.[56–59] However, the typical traditional DOE is static. Therefore, implementing a method that captures interactions among parameters and minimizes the number of experiments is essential to further understand the chemistry. NEXTorch integrates design of experiments (DOE), Bayesian optimization, and surrogate modeling to optimize the function of interest, i.e., objective function.[52] The initial DOE and subsequent sampling points were generated using pyKriging, an open-source kriging software in Python.

Machine learning analysis

Principal Component Analysis (PCA) was carried out using the Minitab software.

Conflicts of interest

The authors are inventors on a patent application on the process described in the manuscript.

Acknowledgments

This work was supported as part of the Catalysis Center for Energy Innovation, an Energy Frontier Research Center funded by the U.S. Department of Energy, Office of Science, and Office of Basic Energy Sciences under award number DE-SC0001004.

References

1. M. A. Perea-Moreno, E. Samerón-Manzano and A. J. Perea-Moreno, *Sustainability*, 2019, **11**, 863.
2. N. Tripathi, C. D. Hills, R. S. Singh and C. J. Atkinson, C. J., *npj Clim. Atmos. Sci.,* 2019, **2**, 35.
3. S. Dutta and B. Saha, *ACS Catal.,* 2017, **7**, 5491–5499.
4. S. Liu, T. R. Josephson, A. Athaley, Q. P. Chen, A. Norton, M. Ierapetritou, J. I. Siepmann, B. Saha and D. G. Vlachos, *Sci. Adv.*, 2019, **5**, eaav548.
5. R. E. Patet, N. Nikbin, L. Williams, S. K. Green, C. Chang, W. Fan, S. Caratzoulas, P. J. Dauenhauer and D. G. Vlachos, *ACS Catal.*, 2015, **5**, 2367–2375.
6. O. A. Abdelrahman, D. S. Park, K. P. Vinter, C. S. Spanjers, L. Ren, H. J. Cho, D. G. Vlachos, W. Fan, M. Tsapatsis and P. J. Dauenhauer, *ACS Sustainable. Chem. Eng.*, 2017, **5**, 3732–3736.
7. D. S. Park, K. E. Joseph, M. Koehle, C. Krumm, L. Ren, J. N. Damen, M. H. Shete, H. S. Lee, X. Zuo, B. Lee, W. Fan, D. G. Vlachos, R. F. Lobo, M. Tsapatsis and P. J. Dauenhauer, *ACS Cent. Sci.*, 2016, **2**, 820–824.
8. M. Fefer, *J. Am. Oil Chem. Soc.*, 1978, **55**, A342–348.
9. V. M. Dembitsky, *Lipids*, 2006, **41**, 309–340.
10. ExxonMobil, Branched alcohols, https://www.exxonmobilchemical.com/en/products/branched-alcohols, (accessed 28 February 2023).
11. C. D. Collins in *Phytoremediation: Methods and Reviews, Vol. 23* (Ed.: N. Willey), Humana Press Inc., Totowa, 2007, pp. 99 – 108.
12. D. R. Bassett, *J. Coat. Technol.*, 2001, **73**, 43–55.
13. ExxonMobil, Branched higher olefins, https://www.exxonmobilchemical.com/en/products/branched-higher-olefins, (accessed 28 February 2023).
14. Paint & Coatings Industry Magazine. Novel 1K and 2K Moisture Curing Vinyl Alkoxysilane Technology, 2019, https://www.pcimag.com/articles/106704-novel-1k-and-2k-moisture-curing-vinyl-alkoxysilane-technology, (accessed 28 February 2023).
15. M. Research, Fatty Amines Market by Type, End Use, Function, Region - Global Forecast to 2024. https://www.marketresearch.com/MarketsandMarkets-v3719/Fatty-Amines-Type-Primary-Secondary-12979635/, (accessed 28 February 2023).
16. W. H. E. Mueller and M. Hartmann, *US Pat.*, US5342979A, Evonik Operations GmbH, 1994.
17. M. Fefer and A. J. Rutkowski, *J. Am. Oil Chem. Soc.*, 1968, **45**, 5–10.
18. R. W. Haushalter, W. Kim, T. A. Chavkin, L. The, M. E. Garber, M. Nhan, P. D. Adams, C. J. Petzold, L. Katz and J. D. Keasling, *Metab. Eng.*, 2014, **26**, 111–118.

19. T. Dulermo, F. Coze, M.-J. Virolle, V. Méchin, S. Baumberger and M. Froissard. *OCL - Oilseeds fats Crops Lipids*, 2016, **23**, A202.

20. E. J. Steen, Y. Kang, G. Bokinsky, Z. Hu, A. Schirmer, A. McClure, S. B. del Cardayre and J. D. Keasling, *Nature*, 2010, **463**, 559–562.

21. X.-L. Li , K. Zhang , J.-L. Jiang , R. Zhu , W.-P. Wu , J. Deng and Y. Fu , *Green Chem.*, 2018, **20**, 362–368.

22. J.-P. Lange, E. van der Heide, J. van Buijtenen and R. Price, ChemSusChem, 2012, **5**, 150–166.

23. Y. Nakagawa, M. Tamura and K. Tomishige. *ACS Catal.*, 2013, **3**, 2655–2668.

24. F. D. Pileidis and M.-M Titirici, *ChemSusChem*, 2016, **9**, 562–582.

25. S. Li, W. Deng, S. Wang, P. Wang, D. An, Y. Li, Q. Zhang and Y. Wang, *ChemSusChem*, 2018, **11**, 1995–2028.

26. A. M. Norton, S. Liu, B. Saha and D. G. Vlachos, *ChemSusChem*, 2019, **12**, 4780–4785.

27. A. Corma, O. de la Torre and M. Renz, *Energy Environ. Sci.*, 2012, **5**, 6328–6344.

28. A. D. Sutton, F. D. Waldie, R. Wu, M. Schlaf, L. A. Silks 3rd and J. C. Gordon, *Nat. Chem.*, 2013, **5**, 428–432.

29. W. Wang, N. Li, S. Li, G. Li, F. Chen, X. Sheng, A. Wang, X. Wang, Y. Cong and T. Zhang, *Green Chem.*, 2016, **18**, 1218–1223.

30. S. Chen and C. Zhao, *ACS Sustainable Chem. Eng.* 2021, **9**, 10818–10826.

31. S. Dutta, A. Bohre, W. Zheng, G. R. Jenness, M. Núñez, B. Saha and D. G. Vlachos, *ACS Catal.*, 2017, **7**, 3905–3915.

32. A. Corma, O. de la Torre, M. Renz and N. Villandier, *Angew. Chem., Int. Ed.*, 2011, **50**, 2375–2378.

33. G. Li, N. Li, Z. Wang, C. Li, A. Wang, X. Wang, Y. Cong and T. Zhang, *ChemSusChem*, 2012, **5**, 1958–1966.

34. S. Liu, R. Bhattacharjee, S. Li, A. Danielson, T. Mazal, B. Saha and D. G. Vlachos, *Green Chem.*, 2020, **22**, 7896–7906.

35. S. Liu, B. Saha and D. G. Vlachos, *Green Chem.*, 2019, **21**, 3606–3614.

36. P. Ferrini, S. F. Koelewijn, J. Van Aelst, N. Nuttens and B. F. Sels, *ChemSusChem*, 2017, **10**, 2249–2257.

37. E. O. Ebikade, S. Sadula, S. Liu and D. G. Vlachos, *Green Chem.*, 2021, **23**, 10090–10100.

38 T. Mochizuki, K. Kakinuma, M. Uchida, S. Deki, M. Watanabe and K. Miyatake, *ChemSusChem*, 2014, **7**, 729–733.

39 C. Wang and S. J. Paddison, *Soft Matter*, 2014, **10**, 819–830.

40 V. S. Likhomanov, O. N. Primachenko and S. S. Ivanchev. *Russ. J. Appl. Chem.*, 2014, **87**, 1314–1318.

41 S. So, H. Kang, D. Choi and K.-H Oh, *Int. J. Hydrogen Energy*, 2020, **45**, 19891–19899.

42 N. Nikbin, S. Caratzoulas and D. G. Vlachos, *ChemSusChem*, 2013, **6**, 2066–2068.

43 M. J. Gilkey, R. Balakumar, D. G. Vlachos and B. Xu, *Catal. Sci. Technol.*, 2018, **8**, 2661–2671.

44 A. V. Tran, S.-K. Park, H. J. Lee, T. Y. Kim, Y. Kim, Y.-W. Suh, K.-Y. Lee and Y. J. Kim, *ChemSusChem*, 2022 **15**, e202200375.

45 H. L. Ngo, R. O. Dunn, B. Sharma and T. A. Foglia, *Eur. J. Lipid Sci. Technol.*, 2011, **113**, 180–188.

46 T. L. Lohr, Z. Li, R. S. Assary, L. A. Curtiss and T. J. Marks, *Energy Environ. Sci.*, 2016, **9**, 550–564.

47 J. Zhou, R. Zhu, J. Deng and Y. Fu, *Green Chem.*, 2018, **20**, 3974–3980.

48 Z. Li, R. S. Assary, A. C. Atesin, L. A. Curtiss and T. J. Marks, *J. Am. Chem. Soc.*, 2013, **136**, 104–107.

49 J. Keskiväli, P. Wrigstedt, K. Lagerblom and T. Repo, *Appl. Catal. A*, 2017, **534**, 40–45.

50 J. Keskiväli, A. Parviainen, k. Lagerblom and T. Repo, *RSC Adv.*, 2018, **8**, 15111–15118.

51 D. R. Parkinson, *Analytical Techniques for Scientists*, Elsevier, 2014.

52 Y. Wang, T.-Y. Chen and D. G. Vlachos, *J. Chem. Inf. Model.*, 2021, **61**, 5312–5319.

53 Q. Xia, Y. Xia, J. Xi, X. Liu, Y. Zhang, Y. Guo and Y. Wang, *ChemSusChem*, 2017, **10**, 747–753.

54 B. A. Ogunnaike, *Random phenomena : fundamentals of probability and statistics for engineers*, CRC Press, Boca Raton, 2010.

55 G. E. P. Box and N. R. Draper, *Empirical model-building and response surfaces*, Wiley, 1987.

56 E. R. Gunawan and D. Suhendra, *Indones. J. Chem.*, 2010, **8**, 83–90.

57 O. O. Awolu and S. K. Layokun, *Int. J. Energy Environ. Eng.*, 2013, **4**, 1–9.

58 L. Zhou, J. Yao, Z. Ren, Z. Yu, and H. Cai, *Energies*, 2020, **13**, 2754.

59 I. G. Moorthy, J. P. Maran, S. Ilakya, S. L. Anitha, S. P. Sabarima and B. Priya, *Ultrason. Sonochem.*, 2017, **34**, 525–530.